

1 **Acknowledgments**

2 This research was supported by the Ministerio de Ciencia e Innovación (Grants: AGL2007-
3 66320-CO2-02/AGR), CSIC (Grants: PIE-200840I214 and 200840I246) and DGA- Obra
4 social La Caixa (Grants: GA-LC-010/2008; GA-LC-006-2008). The authors are grateful to E.
5 Paracuellos, A. Bielsa, J. Salvador and R. Gracia for technical help in several aspects of this
6 study.

1 **TDR pressure cell for monitoring water content retention and bulk electrical**
2 **conductivity curves in undisturbed soil samples**

4 **Abstract**

5 The water retention curve ($\theta(\psi)$), which defines the relationship between soil volumetric
6 water content (θ) and matric potential (ψ), is of paramount importance in characterizing the
7 hydraulic behaviour of soils. However, few methods are so far available for estimating $\theta(\psi)$ in
8 undisturbed soil samples. We present a new design of TDR-pressure cell (TDR-Cell) for
9 estimating $\theta(\psi)$ in undisturbed soil samples. The TDR-Cell consists of a 50-mm-long and 50-
10 mm internal diameter stainless steel cylinder (which constitutes the outer frame of a coaxial
11 line) attached to a porous ceramic disc and closed at the ends with two aluminium lids. A 49-
12 mm-long and 3-mm-diameter stainless steel rod, which runs longitudinally through the centre
13 of the cylinder, constitutes the inner rod of a coaxial TDR probe. The TDR-Cell was used to
14 determine the $\theta(\psi)$ curves of a packed sand and seven undisturbed soil samples from three
15 profiles of agricultural soils. These $\theta(\psi)$ curves were subsequently compared to those obtained
16 from the corresponding 2-mm sieved soils using the pressure plate method. Measurements of
17 bulk electrical conductivity, σ_a , as a function of the water content, $\sigma_a(\theta)$, of the undisturbed
18 soil samples were also performed. An excellent correlation ($R^2 = 0.988$) was found between
19 the θ values measured by TDR on the different undisturbed soils and the corresponding θ
20 obtained from the soil gravimetric water content. A typical bimodal $\theta(\psi)$ function was found
21 for most of the undisturbed soil samples. Comparison between the $\theta(\psi)$ curves measured with
22 the TDR-Cell and those obtained from the 2-mm sieved soils showed that the pressure plate
23 method overestimates θ at low ψ values. The $\sigma_a(\theta)$ relationship was well described by a

- 1 simple power expression ($R^2 > 0.95$), in which the power factor, defined as tortuosity, ranged
- 2 between 1.18 and 3.75.
- 3
- 4 **Keywords:** Time Domain Reflectometry; Volumetric water content; Pressure plate extractor;
- 5 Coaxial cell.

1 **1. Introduction**

2 The relationship between the soil volumetric water content (θ) [m^3m^{-3}] and the matric
3 potential (ψ) [kPa], i.e. the water retention function, $\theta(\psi)$, has become crucial for
4 characterizing the soil hydraulic properties, the key feature for planning and managing new
5 irrigation schemes. The water retention curve is very dependent upon the particle-size
6 distribution, which determines the soil texture, and the arrangement of the solid particles,
7 which refers to the soil structure. The shape of the water retention curve is also dependent on
8 the soil organic matter and the soil water composition (Dane and Hopmans, 2002).

9 Common approaches for estimating $\theta(\psi)$ require paired ψ and θ measurements. The water
10 retention information is commonly obtained by bringing the soil sample to equilibrium by
11 applying a constant pressure gradient across the soil, driving water movement while
12 preventing air entering into a pressurized chamber (Dane and Hopmans, 2002). The θ is
13 generally calculated from the gravimetric water content and the dry bulk density of the soil
14 sample, or in cases where the sample is an undisturbed soil contained in a cylinder, by using
15 the cylinder volume directly. The most common laboratory technique for estimating $\theta(\psi)$ is
16 the pressure plate extractor. A pressure plate extractor referred to as a “Temple cell” is
17 commonly used for suctions up to -100 kPa. For higher matric suctions (typically -1500 kPa)
18 more robust pressure cells are used (Wand and Benson, 2004). Depending on the dimensions
19 of the pressure plate extractor, disturbed or intact soil samples can be used. Measurements of
20 $\theta(\psi)$ in undisturbed soil samples are highly desirable because changes in pore-size distribution
21 caused by sieving soil samples produce substantial changes in $\theta(\psi)$ with respect to its original
22 shape.

23 Time Domain Reflectometry (TDR) is a non-destructive technique that allows simultaneous
24 estimations of the volumetric water content and the bulk electrical conductivity (σ_a). TDR

1 employs a fast-rise signal propagating through a porous medium in order to determine
2 permittivity from travel time, and electrical conductivity from signal attenuation. Water
3 content is inferred from the dielectric measurements due to the large contrast in the
4 permittivity of water compared to the soil and air (Topp and Ferré, 2002). The characteristics
5 of the TDR technique provide a flexible means of measuring θ at multiple locations without
6 requiring soil-specific calibration in many cases. These properties make it possible to combine
7 this technique with a classical pressure plate extractor to estimate $\theta(\psi)$. For instance, Wraith
8 and Or (2001) measured $\theta(\psi)$ of different soils using a combination of a 15-bar pressure plate
9 and a 20-cm-long TDR probe. Jones et al. (2005) designed a 19.6-cm-long TDR coaxial cell to
10 measure water content at adjustable pressure heads without repacking or disturbing the soil
11 sample. More recently, Moret-Fernández et al. (2008) developed a type of pressure cell
12 associated with a zigzag-shaped TDR probe for determining the soil water retention curve in
13 disturbed thin soil samples. However, although this last design reduces the length of the soil
14 cores and, consequently, reduces the risk of soil compression (Grossman and Reinsch, 2002),
15 the zigzag-shaped wires limit the TDR application to disturbed soil samples.

16 The bulk electrical conductivity of soil depends mainly on three variables: (a) the effective
17 θ , (b) the electrical conductivity of the soil solution, and (c) a geometric factor, which
18 accounts for the complex geometry of the soil matrix (Mualem and Friedman, 1991). For
19 unsaturated soils, Rhoades et al. (1976) found that the $\sigma_a(\theta)$ relationship could be satisfactorily
20 described with a polynomial function. However, as subsequently observed by Rhoades et al.
21 (1989), this equation was only valid for σ_a values close to 0.1 S m^{-1} . On the basis of the
22 hypothesis that the tortuosity factor affecting the bulk electrical conductivity is identical to that
23 defined for predicting the soil hydraulic conductivity, Mualem and Friedman (1991) showed

1 that $\sigma_a(\theta)$ could be satisfactorily described using a simple power expression, in which the
2 calibration coefficient was, for most soils, equal to 2.5.

3 The objective of this paper is to present a new design of TDR-pressure cell (TDR-Cell) for
4 estimating $\theta(\psi)$ and $\sigma_a(\theta)$ curves in thin undisturbed soil samples (5-cm high). The TDR-Cell
5 was calibrated in water and soils with different water content and tested in packed sand and in
6 seven different soil samples. The undisturbed $\theta(\psi)$ curves were subsequently compared to
7 those obtained in the corresponding 2-mm sieved soils using a conventional pressure plate
8 method. This comparison will make possible to value the strengths of the TDR-Cell regarding
9 to the pressure plate extractor with disturbed soil samples, which is incorrectly used in many
10 research laboratories to estimate, for instance, the soil water retention curve or the plant
11 available soil water content.

12

13 **2. Theory**

14 *Description of TDR*

15 A TDR system launches an electromagnetic pulse along a transmission line and records a
16 signal or TDR waveform, which is expressed by the voltage (V) or reflection coefficient (ρ) as
17 a function of time (t). The transit time of the TDR pulse propagating one return trip in a
18 transmission line of length L (m) t_L , is represented by

$$19 \quad t_L = \frac{2L\sqrt{\epsilon_a}}{c} \quad (1)$$

20 where c is the velocity of light in free space ($3 \times 10^8 \text{ m s}^{-1}$) and ϵ_a is the apparent permittivity of
21 the medium (Topp and Férré, 2002). Estimations of θ from ϵ_a values are calculated by the
22 Topp and Reynolds (1998) linear calibration form

$$23 \quad \theta = 1.16 \left(\frac{t_s}{t_{air}} \right) - 1.76 \quad (2)$$

1 where t_s and t_{air} are the travel time in soil and air, respectively

2 The voltage reflection coefficient of the TDR waveform, ρ , as a function of time, t , is
3 typically defined as

$$4 \quad \rho(t) = \frac{V(t) - V_0}{V_0 - V_i} \quad -1 \leq \rho \leq +1 \quad (3)$$

5 where $V(t)$ is the measured voltage at time t , V_0 is the voltage in the cable just prior to entering
6 the probe (standard impedance value of 50 Ω), and V_i is the incident voltage of the cable tester
7 prior to the pulse rise. The V_i has a constant value over time and, for our case, it will be
8 assumed to be equal to zero.

9 As an electromagnetic signal propagating in conductive media, the TDR waveform
10 undergoes attenuation. On the basis of the Giese and Tiemann (1975) thin-layer model, Lin et
11 al., (2008) showed that the sample electrical conductivity, σ (S m^{-1}), recorded with an
12 uncoated twin-rod TDR probe, can be related to the long-time attenuation of the TDR signal
13 according to

$$14 \quad \sigma = \frac{K_p}{Z_r} \left(\frac{1 - \rho_{\infty,Scale}}{1 + \rho_{\infty,Scale}} \right) \quad (4)$$

15 where $\rho_{\infty,Scale}$ is the scaled steady-state reflection coefficient corresponding to the ideal
16 condition in which there is no instrument error or cable resistance. Z_r is the output impedance
17 of the TDR cable tester (50 Ω), and K_p (m^{-1}) is the probe-geometry-dependent cell constant
18 value, which can be determined from the probe geometries characteristics or by immersing the
19 probe in different electrolyte solutions of known conductivity (Wraith, 2002). The $\rho_{\infty,SC}$ to be
20 used in the usual Giese–Tiemann equation is calculate according to

$$21 \quad \rho_{\infty,Scale} = 2 \frac{(\rho_{\infty,air} - \rho_{\infty,SC})(\rho - \rho_{\infty,air})}{(1 + \rho_{\infty,SC})(\rho - \rho_{\infty,air}) + (\rho_{\infty,air} - \rho_{\infty,SC})(1 + \rho_{\infty,air})} + 1 \quad (5)$$

1 where ρ , $\rho_{\infty,air}$ and $\rho_{\infty,SC}$ are the steady-state reflection coefficient of the sample under
2 measurement, open in air and short-circuited, respectively

3

4 *Soil water retention curves*

5 The most common function used to describe the soil water retention curve is the unimodal
6 van Genuchten (1980) equation

$$7 \quad \frac{\theta - \theta_r}{\theta_{sat} - \theta_r} = \left[\frac{1}{1 + (\alpha\psi)^n} \right]^m \quad (6)$$

8 where n is the pore-size distribution parameter, $m = 1 - (1/n)$, α [kPa] is the scale factor, and θ_{sat}
9 and θ_r are the saturated and residual volumetric water contents, respectively. Water retention
10 curves for soil with multiple porosity are better approached using the model proposed by
11 Durner (1994), which involves the linear superposition of van Genuchten (1980) subcurves
12 and is expressed as

$$13 \quad \theta = \theta_r + (\theta_{sat} - \theta_r) \sum_{i=1}^k w_i \left[\frac{1}{1 + (\alpha_i\psi)^{n_i}} \right]^{m_i} \quad (7)$$

$$14 \quad 0 < w_i < 1$$

$$15 \quad \sum w_i = 1$$

$$16 \quad \alpha_i > 0, m_i > 0, n_i > 1$$

17 where k is the total number of i “subsystems” that form the total pore-size distribution, and w_i
18 is a weighting factor for the subcurves.

19

20

21

1 *Water content vs. bulk electrical conductivity curves*

2 The σ_a of a soil can be considered to consist of two components: (i) the contribution of ions
3 in soil particles, and (ii) the contribution of ions in the soil solution (Nadler and Frenkel,
4 1979). The $\sigma_a(\theta)$ relationship was first described by Rhoades et al. (1976) as

$$5 \quad \sigma_a(\theta) = \sigma_w \theta T + \sigma_s \quad (8)$$

6 where σ_w and σ_s are the electrical conductivity of the soil solution and the solid phase
7 conductivity, respectively, and $T = a\theta + b$, with a and b being empirical coefficients.
8 Alternatively, on the basis of the hypothesis that the tortuosity factor accounting for the
9 reduction in hydraulic conductivity is identical to the tortuosity factor reducing the soil
10 solution electrical conductivity, Mualem and Friedman (1991) found that $\sigma_a(\theta)$ could be
11 described with a simple power function (neglecting σ_s) as

$$12 \quad \sigma_a = \sigma_{a-sat} \left(\frac{\theta}{\theta_{sat}} \right)^\beta \quad (9)$$

13 where σ_{a-sat} is the soil bulk electrical conductivity at saturation and β is a tortuosity factor that,
14 dependent on the soil's water transmission porosity, defines the rate of decrease between σ_a
15 and θ .

16

17 **3. Material and methods**

18 *Description of the TDR-Cell*

19 The pressure head TDR-Cell consists of a commercially available stainless steel cylinder
20 (50-mm long and 50-mm in internal diameter), commonly used to estimate soil bulk density,
21 joined through the base to a commercially available porous ceramic disc (7-mm thick and 50-
22 mm in diameter) and hermetically closed at the ends with two aluminium single-hole drilled
23 lids (Fig. 1). A 49-mm-long and 3-mm-diameter stainless steel rod, which was vertically

1 inserted in the upper lid of the TDR-Cell, runs longitudinally along the axis at the centre of the
2 stainless steel cylinder. This rod is connected to the inner wire of a female BNC connector,
3 which is glued onto the upper lid of the TDR pressure cell. The two elements, the stainless
4 steel rod and the cylinder, form a cylindrical coaxial line of 49-mm length and 50-mm internal
5 diameter. Two aluminium rings attached to several rubber joints hermetically close the lids of
6 the TDR-Cell against the stainless steel cylinder (Fig. 1). The TDR-Cell is connected to a TDR
7 cable tester (Campbell TDR100) by a 1.2-m-long RG 58 coaxial cable of 50 Ω nominal
8 impedance, and the TDR signals are transferred to a computer that records and analyses the
9 TDR waveforms using the software TDR-Lab V.1.0 (Moret-Fernández et al., 2010). The TDR
10 volumetric water content (θ_{TDR}) and the bulk electrical conductivity (σ_a) are estimated using
11 the Topp and Reynolds (1998) (Eq. 2) and Lin et al. (2008) (Eq. 4) models, respectively.

12

13 *TDR-Cell testing and experimental design*

14 A first laboratory experiment was performed to calibrate the effective length and the cell
15 constant (K_p) (Eq. 4) of the TDR coaxial probe. The effective length was calculated with the
16 TDR-Lab software by immersing the coaxial probe in distilled water, and the K_p was
17 determined by immersing the probe in different electrolyte solutions of known conductivity
18 (Moret-Fernández et al., 2010). Additionally, the theoretical K_p value was also calculated.
19 Although the probe constant for a purely coaxial cell can be calculated analytically, the
20 specific geometry of the TDR-Cell, in which the effect of the top and bottom metallic flanges
21 are not negligible, makes necessary to calculate K_p by means of numerical methods. To this
22 end a commercial finite elements modelling software (COMSOL Multiphysics
23 <http://www.comsol.com/>) was used. In a two-dimensional axisymmetric mode, the cell
24 nominal geometry was finely meshed to approximately 40000 nodes and the subsequent DC
25 conductivity problem was solved. The viability of the TDR-Cell for estimating water retention

1 curves ($\theta(\psi)$) was tested in sand (average grain size of 80-160 μm) and in seven different
2 undisturbed soil samples. The gypsum of the soil samples was titrated by the loss of crystal
3 water from the gypsum, in accordance with Artieda et al. (2006). The undisturbed soil samples
4 were taken, using the core method (Grossman and Reinsch, 2002), from the genetic horizons
5 of three different pits (Table 1) opened for soil profile study. Two replications were performed
6 per soil horizon. The preparation of the soil samples required the following phases. In a first
7 step, the surfaces of the undisturbed soil core were carefully levelled with a scraper. The
8 bottom of the core was covered with a nylon base (20- μm mesh) which, glued to a stainless
9 steel open ring, was inserted at the bottom of the cylinder. Using a power drill, a 3-mm-
10 diameter and 45-mm-long hole was drilled longitudinally through the top and down the centre
11 of the undisturbed soil sample. The stainless steel rod of the TDR-Cell was inserted in the
12 drilled hole, and the top of the TDR-Cell was hermetically closed by screwing the upper
13 aluminium ring to the upper TDR-Cell lid (Fig. 1). A dry ceramic disc was placed on the
14 bottom lid of the TDR-Cell, and the stainless steel core plus the upper TDR-Cell lid were
15 attached to the ceramic disc. The system was finally hermetically closed by screwing the lower
16 aluminium ring to the bottom lid of the TDR-Cell. A first measurement of θ_{TDR} was performed
17 in air-dry soil conditions, which have been calculated to correspond to a soil pressure head of
18 about 166 MPa (Munkholm and Kay, 2002). Next, the soil sample was saturated by injecting
19 distilled water through the base of the TDR-Cell, and the soil was considered saturated when
20 the water started to leave via the top of the pressure cell. Once the soil was saturated, pressure
21 steps were sequentially applied at 1.7, 3, 5, 10, 50, 100, 500, and 1500 kPa. Ceramic plates
22 (Soil Moisture Inc. UK) with bubbling pressures of -0.5, -3 and -5 bar (Soil Moisture Inc. UK)
23 were used to regulate the outlet water flow for pressure heads up to 50, 100 and 500 kPa,
24 respectively. The outlet water flow at a pressure head of 1500 kPa was regulated using a
25 cellophane membrane plus a -0.5 bar ceramic plate system. Values of θ_{TDR} and σ_a were

1 recorded at soil saturation, and 24, 48 and 72 hours after starting each pressure head step for ψ
2 values up to -100, -500 and -1500 kPa, respectively. Preliminary measurements of θ_{TDR}
3 performed in the BU7-Ap and BU7-R1 soil cores at 500 and 1500 kPa of pressure heads and
4 24 h of time intervals during 4 days showed that 48 and 72 h were enough to reach the soil the
5 respective water equilibrium.

6 The $\theta(\psi)$ curves were fitted to the unimodal (van Genuchten, 1980) or bimodal functions
7 (Durner, 1994) using SWRC Fit Version 1.2 software (<http://seki.webmasters.gr.jp/swrc/>)
8 (Seki, 2007). The gravimetric water content (W) of the different undisturbed soil samples was
9 measured in air-dry conditions and at pressure heads up to -50 kPa, and the corresponding
10 volumetric water contents (θ_w) were calculated from W and the undisturbed soil dry bulk
11 density (ρ_b). The dry bulk density of the undisturbed soil samples was calculated as the soil
12 weight dried at 50 °C for 72 hours divided by the soil volume. Since gypsum content was
13 relevant in the studied soils, the 50°C temperature was used to avoid the constitutional water
14 release by the gypsum crystal because of the transformation of gypsum into bassanite or
15 anhydrite at temperatures > 50°C (Nelson et al., 1978; Artieda et al., 2006; Lebron et al., 2009;
16 Herrero et al., 2009). Accounting these water molecules as moisture would be erroneous;
17 moreover the “dry” weight of the “cooked” soil at 105°C would also differ from the true
18 weight of the naturally dry gypsum, flawing further determinations related to weight.

19 The different undisturbed soil $\theta(\psi)$ curves estimated with the TDR-Cell were compared to
20 the corresponding curves measured for disturbed soil samples using a conventional pressure
21 plate method (Table 1). The air-dry soil samples were ground, sieved at 2-mm diameter, and
22 poured into 5-cm internal diameter and 0.4-cm thick rubber rings, which were placed on the
23 ceramic plate of the pressure plate apparatus. The soil samples were wetted to saturation and
24 pressure steps were sequentially applied at 1.7, 3, 5, 10, 50, 100, 500, and 1500 kPa. A new

1 disturbed soil sample was used for each pressure head, and W was measured 24 hours after
2 starting each pressure head step. The volumetric water content of the disturbed soil samples
3 was calculated as the gravimetric water content (W) multiplied by the ρ_b of the sieved soil
4 samples (Table 1). Two replications of the water content measurements were performed per
5 pressure head and sampling point.

6

7 **4. Results and discussion**

8 The effective length and theoretical and experimental K_p values calculated for the coaxial
9 probe used in the TDR-Cell were 5.14 cm, and 7.29 and 6.38 m⁻¹, respectively. The 12%
10 discrepancy between the experimental and theoretical K_p values can be considered as a good
11 approximation for a calculation derived from nominal simplified geometry parameters. The
12 good correlation ($R^2 = 0.988$) and the low RMSE (RMSE = 0.017) found between the θ_{TDR}
13 values measured for the packed sand and for the different undisturbed soil samples and
14 pressure heads (in air-dry soil conditions and with ψ ranging between 0 and -0.5 bar) and the
15 corresponding θ_w indicate that the coaxial TDR probe used in this experiment is accurate
16 enough to estimate the volumetric water content (Fig. 2).

17 The ρ_b measured in the sand sample was 1.47 g cm⁻³ and the $\theta(\psi)$ obtained with the TDR
18 pressure cell showed a typical van Genuchten (1980) unimodal function (Fig. 3), with an
19 excellent fit between the measured and modelled $\theta(\psi)$ (Table 2). The undisturbed soil samples
20 used in the experiment had loam to silty clay loam textures, and ρ_b ranged from 1.21 g cm⁻³
21 for the upper soil horizons to 1.70 g cm⁻³ for the deeper ones (Table 1). Assuming a $\theta_r = 0$, the
22 $\theta(\psi)$ estimated with the TDR-Cell shows a double hump for all the undisturbed samples,
23 which indicates that the soils presented a relevant double pore-size distribution. In these cases,
24 a significant w_l value (Eq. 7) was observed (Table 2). Figure 3 shows an example of the

1 unimodal and bimodal $\theta(\psi)$ functions obtained for the sand and the second replication of the
2 BU 7-R2 soil, respectively.

3 Significant differences were observed between the $\theta(\psi)$ functions estimated with the TDR-
4 Cell for undisturbed soil samples, $\theta(\psi)_{TDR}$, and the corresponding curves obtained with the
5 pressure plate method, $\theta(\psi)_{PPM}$ (Fig. 4). Overall, $\theta(\psi)_{PPM}$ presented a significantly higher
6 volumetric water content for the soil macropore range ($\psi > -10$ kPa) (Kay and
7 VandenBygaart, 2002), which should be attributed to the different structural characteristics
8 between the undisturbed and the 2-mm sieved soil samples. As noted by Ahuja et al. (1998),
9 the larger porosity in loose soil, which is related to a lower ρ_b (Rab, 2004; Moret and Arrúe,
10 2007), is generally associated with an increase in soil water retention at the wet end of the
11 $\theta(\psi)$ curve (i.e. pores corresponding to $\psi > -6$ kPa). In contrast, for pressure heads higher than
12 100 kPa, a significantly higher volume of mesopores ($-10 > \psi > -1400$ kPa) was observed in
13 the compacted undisturbed soil samples. As compared to the sieved soils, the extremely high
14 ρ_b observed in some undisturbed soil samples (Table 1) (i.e. the “BU9 Cy” soil which came
15 from a lutitic horizon) should increase the fraction of micropores ($\psi > -1400$ kPa), and
16 consequently enhance the water content at permanent wilting point (-1500 kPa) (Fig. 4). The
17 similar average and standard deviation values found between the gravimetric water content
18 measured with the pressure plates (W_{PPM}) at low pressure heads (from 100 to 1500 kPa) and
19 the corresponding values estimated for the undisturbed soils with the TDR-Cell (W_{TDR})
20 (calculated as the quotient between θ_{TDR} and the undisturbed ρ_b) (Table 3) indicate that the
21 TDR-Cell satisfactorily approaches the $\theta(\psi)$ section corresponding to the soil’s textural
22 properties.

23 As described in the literature (Rhoades et al., 1976; Mualem and Friedman, 1991), the bulk
24 electrical conductivity increased with the volumetric water content (Fig. 5). The high electrical

1 conductivity around saturation found in the BU 7-R2, BU 9-Cy, and BU 10-Ap and By soil
2 samples can be related to the high gypsum content measured in these soil horizons (Table 1).
3 The electrical conductivity of the air-dry soils, which would correspond to the apparent
4 electrical conductivity of the solid phase of the soil (σ_s) (Eq. 8) (Rhoades et al., 1976), was in
5 all cases negligible. Preliminary analysis of the $\sigma_a(\theta)$ relationship showed that the polynomial
6 function proposed by Rhoades et al. (1976) (Eq. 8), which presented incongruent negative b
7 coefficients in some cases (i.e. BU 9-Cy, BU 10-Ap, and BU 10-By), was not appropriate for
8 describing the relationship between the bulk electrical conductivity and the volumetric water
9 content. These results agree with Rhoades et al. (1989), who concluded that the simplified
10 polynomial model (Eq. 8) was valid for σ_a values above approximately 0.1 S m^{-1} . However, an
11 excellent fit was found between the experimental and the modelled Mualem and Friedman
12 (1991) $\sigma_a(\theta)$ curves (Eq. 9) (neglecting σ_s) (Table 4). However, unlike Mualem and Friedman
13 (1991), who found a β value close to 2.5 for both consolidated and unconsolidated coarse
14 soils, the β parameter obtained in this study ranged between 1.18 and 3.75. Since all
15 measurements have been performed on undisturbed soil samples, with bulk densities ranging
16 from 1.24 to 1.70 g cm^{-3} , these results indicate that the β factor was largely affected by the
17 structural characteristics of the soils. No clear correlation ($R^2 = 0.17$) between the β factor and
18 the soil bulk density was found.

19

20 **5. Conclusions**

21 This paper presents a new design of TDR-pressure cell (TDR-Cell) for estimating $\theta(\psi)$ and
22 $\sigma_a(\theta)$ curves on 5-cm-high undisturbed soil samples. The TDR-Cell was tested with different
23 soils, and the $\theta(\psi)$ curves were compared with the corresponding curves obtained with 2-mm
24 sieved soils using the conventional pressure plate method. The results show that the TDR-Cell

1 measures θ satisfactorily. Thus, these results indicate that the proposed TDR-Cell is, in
2 comparison to the pressure plate extractor, a significant advance in estimating the $\theta(\psi)$ and
3 $\sigma_a(\theta)$ functions in undisturbed soil samples. However, some caution is due for the time
4 selected to achieve the water equilibrium in the soil bulk at the largest pressure heads, since
5 the 48 and 72 h used at 500 and 1500 kPa of pressure head may be insufficient for fixed clayey
6 soils. On the other hand, further efforts should be made to improve the TDR-Cell design, using
7 a single ceramic plate for all ranges of pressure heads. This could be achieved by replacing the
8 different ceramic plates that regulate the outlet water flow by a single -0.5 bar ceramic disc
9 plus an adjustable valve running up to a pressure head of -15 bar. In addition, these results
10 open the door to further research studying the relationship between the β factor and the
11 tortuosity parameter of the hydraulic conductivity curves.

12

13 **References**

- 14 Ahuja, L.R., Fiedler, F., Dunn, G. H., Benjamin, J. G., Garrison, A., 1998. Changes in soil
15 water retention curves due to tillage and natural reconsolidation. *Soil Science Society of*
16 *America Journal* **62**: 1228-1233.
- 17 Artieda, O., Herrero, J., Drohan, P.J. 2006. A refinement of the differential water loss method
18 for gypsum determination in soils. *Soil Science Society of America Journal* **70**: 1932-1935.
- 19 Artieda, O., Herrero, J., Drohan, P.J., 2006. A refinement of the differential water loss method
20 for gypsum determination in soils. *Soil Science Society of America Journal* **70**: 1932-1935.
- 21 Dane, J.H., Hopmans, J.W., 2002. Water retention and storage. In, *Methods of Soil Analysis*.
22 Part 4. (Ed. J.H. Dane and G.C. Topp), SSSA Book Series No. 5. Soil Science Society of
23 America, Madison WI.

- 1 Durner, W., 1994. Hydraulic conductivity estimation for soils with heterogeneous pore
2 structure. *Water Resources Research* **30**: 211-223.
- 3 Giese, K., Tiemann, R., 1975. Determination of the complex permittivity from thin-sample
4 time domain reflectometry: Improved analysis of the step response waveform. *Advances in*
5 *Molecular Relaxation Processes* **7**: 45-49.
- 6 Grossman, R.B., Reinsch, T.G., 2002. Bulk density and linear extensibility. In, *Methods of*
7 *Soil Analysis. Part 4.* (Eds. J.H. Dane and G.C. Topp), SSSA Book Series No. 5. Soil
8 Science Society of America, Madison WI.
- 9 Herrero, J., Artieda, O., Hudnall, W.H. 2009. Gypsum, a tricky material. *Soil Science Society*
10 *of America Journal* **73**: 1757-1763.
- 11 Jones, S.B., Mace, R.W., Or, D., 2005. A time domain reflectometry coaxial cell for
12 manipulation and monitoring of water content and electrical conductivity in variable
13 saturated porous media. *Vadose Zone Journal* **4**: 977-982.
- 14 Kay, B.D., VandenBygaart, A.J., 2002. Conservative tillage and depth stratification of
15 porosity and soil organic matter. *Soil and Tillage Research* **66**: 107-118.
- 16 Lebron, I., Herrero, J., Robinson, D.A. 2009. Determination of gypsum content in dryland
17 soils exploiting the gypsum-bassanite phase change. *Soil Science Society of America*
18 *Journal* **73**: 403-411.
- 19 Lin, C-P., Chung, C.C., Huisman, J.J., Tang, S.H., 2008. Clarification and calibration of
20 reflection coefficient for electrical conductivity measurement by Time Domain
21 Reflectometry. *Vadose Zone Journal* **72**: 1033-1040.
- 22 Moret, D., Arrúe, J.L., 2007. Dynamics of soil hydraulic properties during fallow as affected
23 by tillage. *Soil and Tillage Research* **96**: 103-113.

- 1 Moret-Fernández, D., Arrúe, J.L., Pérez, V., López, M.V., 2008. A TDR-pressure cell design
2 for measuring the soil water retention curve. *Soil and Tillage Research* **100**: 114-119.
- 3 Moret-Fernández, D., Vicente, J., Lera, F., Latorre, B., López, M.V., Blanco, N., González-
4 Cebollada, C., Arrúe, J.L., Gracia, R., Salvador, M.J., Bielsa, A., 2010. - TDR-Lab
5 Version 1.0 Users Guide (<http://digital.csic.es/handle/10261/35790>).
- 6 Mualem, Y., Friedman, S.P., 1991. Theoretical prediction of electrical conductivity in
7 saturated and unsaturated soil. *Water Resources Research* **27**: 2771-2777.
- 8 Munkholm, L.J., Kay, B.D., 2002. Effect of Water Regime on Aggregate-tensile Strength,
9 Rupture Energy, and Friability. *Soil Science Society of America Journal* **66**: 702-709.
- 10 Nadler, A., Frenkel, H., 1979. Determination of soil solution electrical conductivity from bulk
11 soil electrical conductivity measurements by the four-electrode method. *Soil Science*
12 *Society of America Journal* **44**: 1261-1221.
- 13 Nelson, R.E., L.C. Klameth, Nettleton, W.D. 1978. Determining soil gypsum content and
14 expressing properties of gypsiferous soils. *Soil Science Society of America Journal*
15 **42**:659–661.
- 16 Rab, M.A., 2004. Recovery of soil physical properties from compaction and soil profile
17 disturbance caused by logging of native forest in Victorian Central Highlands, Australia.
18 *Forest Ecology Manag.* 191, 329–340.
- 19 Rhoades, J.D., Manteghi, N.A., Shouse, P.J., Alves, W.J., 1976. Soil electrical conductivity
20 and soil salinity: new formulations and calibrations. *Soil Science Society of America*
21 *Journal* **53**: 433-439.
- 22 Rhoades, J.D., Manteghi, N.A., Shouse, P.J., Alves, W.J., 1989 Soil electrical conductivity
23 and soil salinity:new formulations and calibration. *Soil Science Society of America Journal*
24 **52**: 433-439.

- 1 Seki, K., 2007. SWRC fit – a nonlinear fitting program with a water retention curve for soils
2 having unimodal and bimodal pore structure. *Hydrological and Earth System Science* **4**:
3 407-437.
- 4 Topp, G.C., and W.D. Reynolds. 1998. Time domain reflectometry: A seminal technique for
5 measuring mass and energy in soil. *Soil Tillage Research* **47**:125-132
- 6 Topp, G.C., Ferré, T.P.A., 2002. Water content, In, Methods of Soil Analysis. Part 4. (Ed. J.H.
7 Dane and G.C. Topp), SSSA Book Series No. 5. Soil Science Society of America,
8 Madison WI.
- 9 Wand, X., Benson, C.H., 2004. Leak-free pressure plate extractor for measuring the soil water
10 characteristic curve. *Geotechnical Testing Journal* **27**: 1-9.
- 11 van Genuchten, M.T., 1980. A closed-form equation for predicting the hydraulic properties of
12 unsaturated soils. *Soil Science Society of America Journal* **44**: 892-898.
- 13 Wraith, J.M., 2002. Time Domain Reflectometry. p. 1289-1297. In J.H. Dane and G.C. Topp
14 (eds.) Methods of Soil Analysis: Part IV Physical Methods. SSSAJ Madison, WI.
- 15 Wraith J.M., Or, D., 2001. Soil water characteristic determination from concurrent water
16 content measurements in reference porous media. *Soil Science Society of America Journal*
17 **65**: 1659-1666.
- 18

Figure captions

1
2
3
4
5
6
7
8
9
10
11
12
13
14
15
16
17
18
19
20
21
22
23

Figure 1. Schematic diagram of the proposed TDR pressure cell.

Figure 2. Correlation between the volumetric water content measured with the TDR-Cell (θ_{TDR}) in sand samples and in different undisturbed soil samples and the corresponding values calculated from the soil gravimetric water content and the dry bulk density of the undisturbed soil (θ_W).

Figure 3. Water retention curves measured with the TDR-Cell (points) in sand and in the second replication of the BU 7-R2 soil and the corresponding modelled unimodal and bimodal functions (lines).

Figure 4. Comparison between the water retention curves measured with the TDR-Cell in the two replications of undisturbed soil samples, and the corresponding average curves measured in the 2-mm sieved soil samples using the pressure plate method (PPM).

Figure 5. Comparison between the measured (points) and modelled (lines) (Eq. 8) soil volumetric water content vs. bulk electrical conductivity relationships obtained for different undisturbed soil samples (Table 1).

1
2
3
4

Table 1. Characteristics of the 2-mm sieved and undisturbed soil samples used to test the pressure head TDR-Cell

Trench	Genetic horizon	Depth cm	2-mm sieved soil bulk density g cm ⁻³	Undisturbed soil bulk density	Gypsum content	Sand	Silt	Clay	Texture
						%			
BU-7	A _p	0-30	1.07	1.23	5.0	6.6	30.1	63.3	Silty clay loam
	R1	40-60	1.22	1.59	10.5	35.8	23.3	40.9	Loam
	R2	60-160	1.15	1.70	20.0	1.7	28.2	70.1	Silty clay loam
BU-9	A _p	0-30	1.03	1.21	6.1	7.4	35.8	56.9	Silty clay loam
	C _y	30-160	1.11	1.68	22.2	1.7	34.4	63.9	Silty clay loam
BU-10	A _p	0-30	1.00	1.24	17.3	7.4	35.7	56.9	Silty clay loam
	B _y	30-100	1.00	1.52	26.8	3.1	36.7	60.3	Silty clay loam

5
6
7

1 **Table 2.** Parameters defining the unimodal (Eq. 5) and bimodal (Eq. 6) water retention curves estimated in packed sand and in different
2 undisturbed soil samples (Table 1), and the coefficient of determination (R^2) for the best fit between the measured and modelled volumetric
3 water content vs. soil pressure head.

Soil sample	Soil horizon	Replication	Model	θ_s	θ_r	w_l	α_l	n_l	α_2	n_2	R^2
				$\text{m}^3 \text{m}^{-3}$							
Sand		1	Unimodal	0.39	0.09	-	0.41	5.48			0.99
BU 7	A _p	1	Bimodal	0.43	≈ 0	0.47	0.31	1.90	$6.7 \cdot 10^{-4}$	1.32	0.99
		2	Bimodal	0.48	≈ 0	0.42	0.25	1.88	$6.0 \cdot 10^{-4}$	1.33	0.99
	R1	1	Bimodal	0.46	≈ 0	0.20	3.36	1.27	0.012	1.19	0.97
		2	Bimodal	0.44	≈ 0	0.45	0.41	1.19	$1.4 \cdot 10^{-5}$	3.14	0.99
	R2	1	Bimodal	0.47	≈ 0	0.33	0.10	1.27	$2.4 \cdot 10^{-4}$	1.56	0.99
		2	Bimodal	0.39	≈ 0	0.26	0.34	1.91	$9.8 \cdot 10^{-4}$	1.31	0.99
BU 9	A _p	1	Bimodal	0.51	≈ 0	0.66	1.44	1.24	$6.8 \cdot 10^{-4}$	1.29	0.99
		2	Bimodal	0.49	≈ 0	0.38	0.33	2.92	$9.4 \cdot 10^{-3}$	1.21	0.99
	C _y	1	Bimodal	0.43	≈ 0	0.04	27.87	38.97	$1.4 \cdot 10^{-3}$	1.22	0.99
		2	Bimodal	0.44	≈ 0	0.20	0.03	1.23	$1.4 \cdot 10^{-4}$	1.32	0.99
BU 10	A _p	1	Bimodal	0.49	≈ 0	0.30	0.15	3.07	$8.9 \cdot 10^{-4}$	1.35	0.99
		2	Unimodal	0.48	≈ 0	0.19	0.086	3.03	$1.0 \cdot 10^{-4}$	1.52	0.99
	B _y	1	Bimodal	0.51	≈ 0	0.25	0.085	3.21	$7.4 \cdot 10^{-5}$	1.74	0.99
		2	Bimodal	0.49	≈ 0	0.59	0.63	1.15	$2.4 \cdot 10^{-4}$	3.17	0.99

4

1
2 **Table 3.** Average and standard deviation (SD) values of the gravimetric
3 water content measured in all soil samples with the pressure plate method
4 (W_{PPM}) and corresponding values calculated with the TDR-Cell (W_{TDR}).

5

Pressure head	W_{PPM}		W_{TDR}	
	Average	SD	Average	SD
kPa	$\text{m}^3 \text{m}^{-3}$			
0.01	0.615	0.067	0.358	0.088
1.7	0.498	0.063	0.331	0.084
3	0.488	0.048	0.329	0.088
5	0.447	0.044	0.308	0.082
10	0.416	0.050	0.291	0.076
50	0.332	0.056	0.257	0.059
100	0.268	0.057	0.240	0.062
500	0.217	0.048	0.234	0.061
1500	0.192	0.057	0.214	0.079

6

1 **Table 4.** Parameters defining the simple power equation (Eq. 7) relating the volumetric water content with the bulk electrical conductivity for
 2 the first (R_1) and the second (R_2) soil replications of the different undisturbed soil samples (Table 1). R^2 and RMSE: coefficient of
 3 determination and root mean square error for the best fit between the measured and modelled volumetric water content vs. bulk electrical
 4 conductivity.

Trench	Genetic horizon	σ_{sat}		β		θ_{sat}		R^2		RMSE	
		R_1	R_2	R_1	R_2	R_1	R_2	R_1	R_2	R_1	R_2
		$S\ m^{-1}$				$m^3\ m^{-3}$					
BU 7	Ap	0.045	0.055	1.180	1.381	0.45	0.47	0.99	0.98	0.005	0.001
	R1	0.110	0.099	1.609	1.615	0.45	0.45	0.98	0.98	0.002	0.001
	R2	0.220	0.073	3.267	1.900	0.46	0.39	0.91	0.94	0.015	0.002
BU 9	Ap	0.053	0.039	1.350	1.397	0.51	0.49	0.96	0.98	0.001	0.001
	Cy	0.133	0.190	2.770	3.753	0.43	0.44	0.99	0.98	0.002	0.031
BU 10	Ap	0.400	0.649	2.133	2.322	0.50	0.49	0.96	0.97	0.008	0.017
	By	0.472	0.699	2.421	3.594	0.52	0.49	0.95	0.96	0.013	0.017

5
6

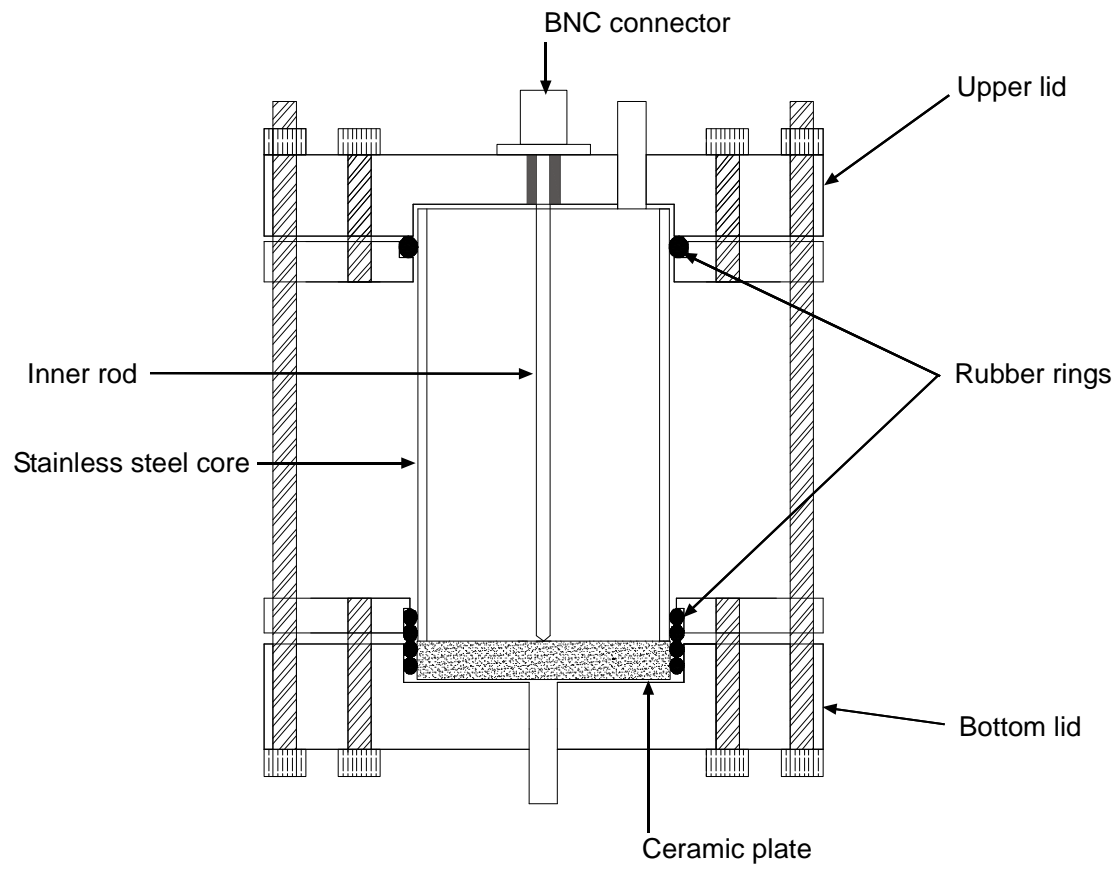


Fig. 1

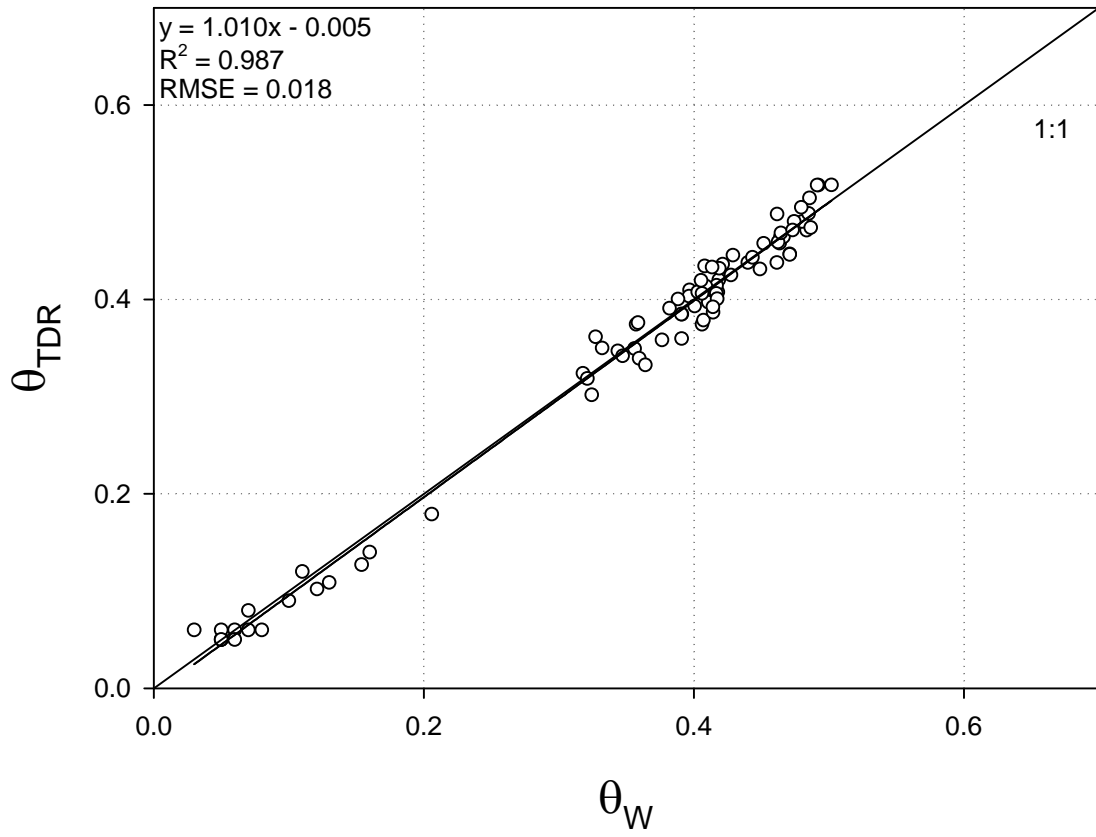


Fig. 2

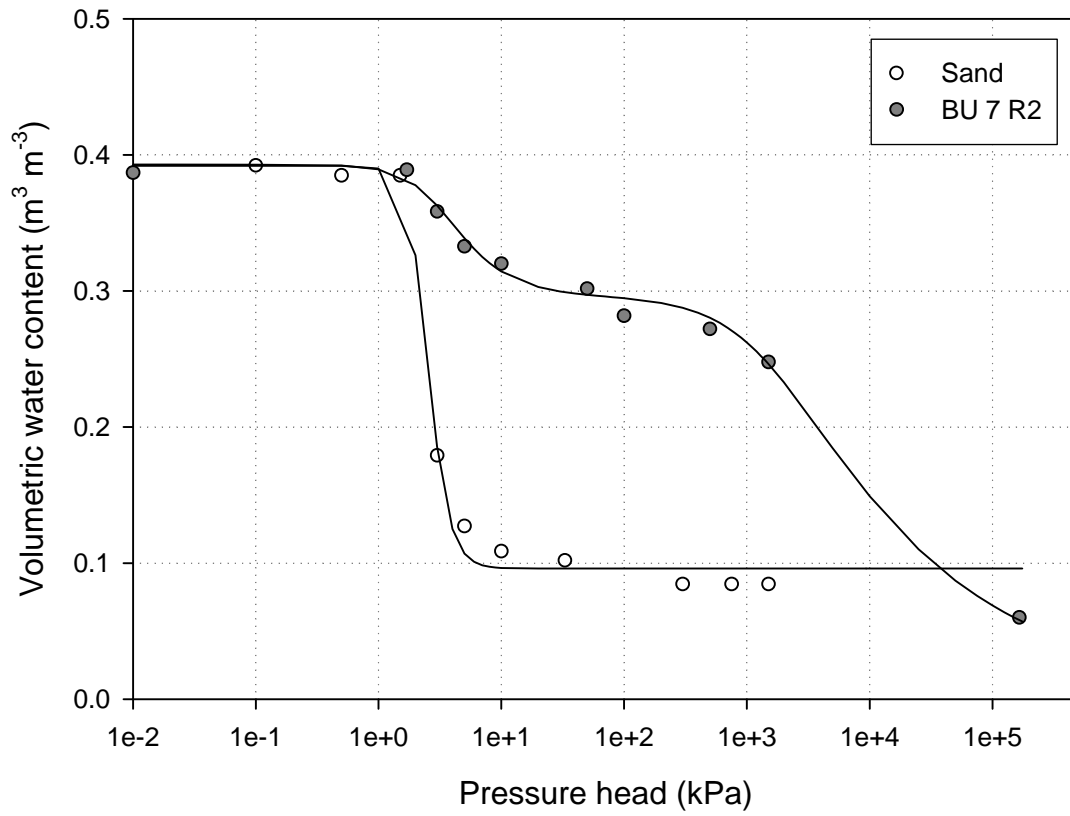


Fig. 3

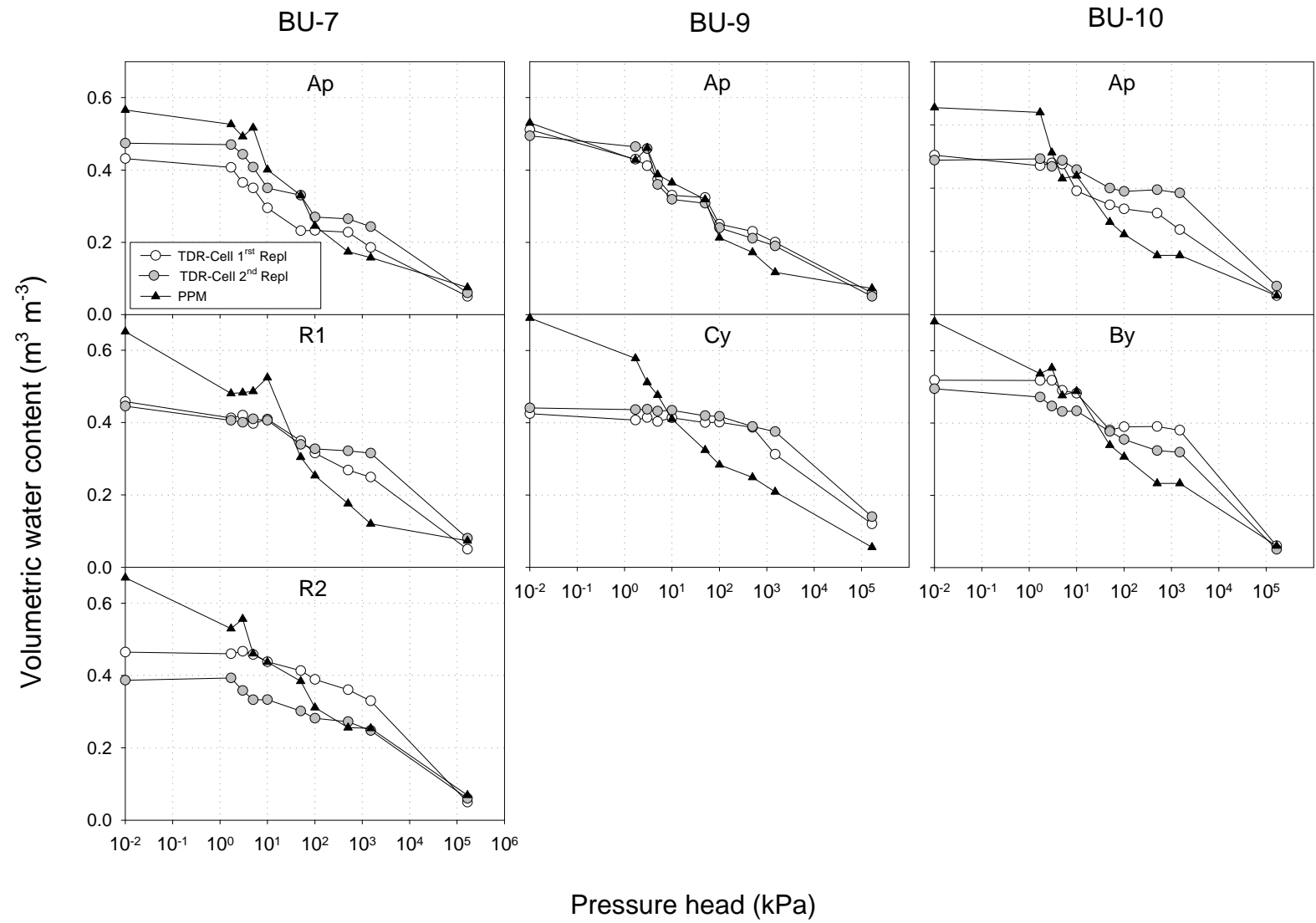


Fig. 4

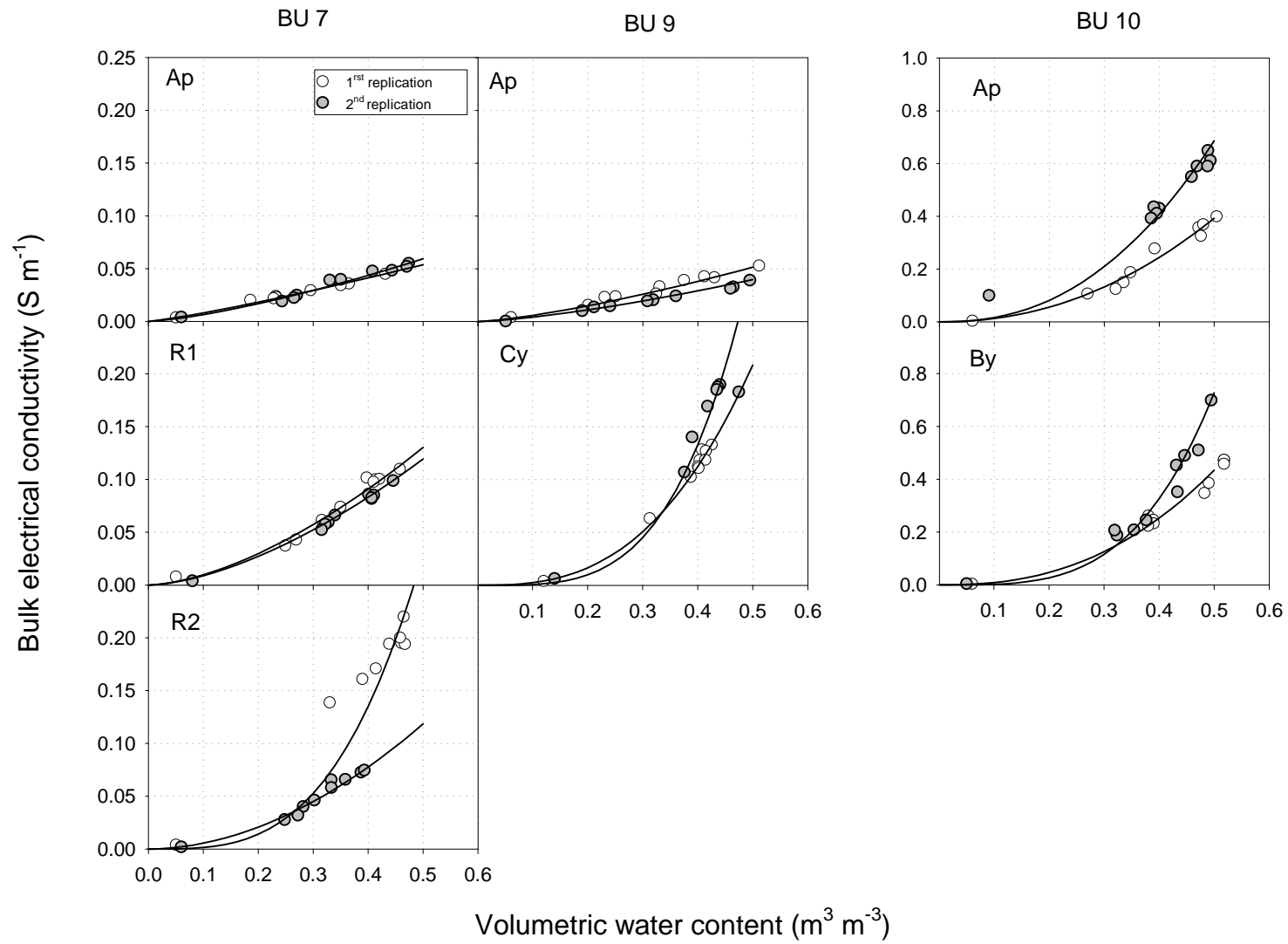


Fig. 5